Block-based streaming blind deconvolution for space-variant turbulence mitigation

David G. Sheppard[a], Amber L. Iler[a], and Bobby R. Hunt[a]
[a]KBR, Inc.

ABSTRACT

This paper extends our 2021 KBR Technical Journal findings on local resolution imagery characteristics in the face of atmospheric turbulence [1] to the applied case of turbulence mitigation. Herein, a block-based, streaming, multi-frame blind deconvolution (MFBD) mitigation method is presented for restoration of imagery impacted by space-variant atmospheric turbulence. An incremental approach is taken, referred to as "streaming", which operates on each new frame as it arrives. For each new frame, an optimization is initiated to minimize the error between the new frame and forward modeling of the object and point spread function (PSF). To adapt to space-variant turbulence conditions, the fundamental units of operation are small, overlapping blocks of pixels extracted from the entire frame. The optimization for each new block is seeded using the solution from the same block area in the previous frame to produce a cumulative, improved, block solution. For each block, the algorithm implements stochastic gradient descent, and alternates between seeking a solution for the PSF and the object, while holding the other constant. To assist in regularizing the PSF solutions during the processing, the PSF estimate is projected onto a sparse dictionary representation of PSFs. The block solutions are combined using an overlap/add method to produce the object estimate after each frame. Our method can utilize either a Picard iterative process or a limited memory Broyden-Fletcher-Goldfarb-Shanno (L-BFGS) algorithm with bound constraints. A comparison of results is presented using data simulated with high-fidelity to real systems and environments. While incremental methods for blind deconvolution have been reported in the literature, our method has been developed explicitly for the routine mechanics of blind deconvolution.

Keywords: atmospheric turbulence, blind deconvolution, block-based image processing, L-BFGS, stochastic gradient descent

1. INTRODUCTION

Image acquisition through optical paths in the atmosphere encounters the macro- and microstructure of the atmospheric medium. This structure consists of large-scale variations in the density, moisture, temperature, and motion of atmospheric constituents, as illustrated in Figure 1. The result of these large- and small-scale atmospheric variations is corresponding variations in the index of refraction along an optical path in the atmosphere. A plane wave launched into the atmosphere has its flat, planar structure altered into a surface of complex and unpredictable contours. This distortion and its effect on the formation of an image by an optical system can be severe, yet common optical design assumptions develop the structure of optical reflections and refractions on the basis of a plane-wave entering the pupil of the optical device. In reality, the distorted wavefront results in the formation of an image that significantly misrepresents the scene that was the source of the original optical information [2].

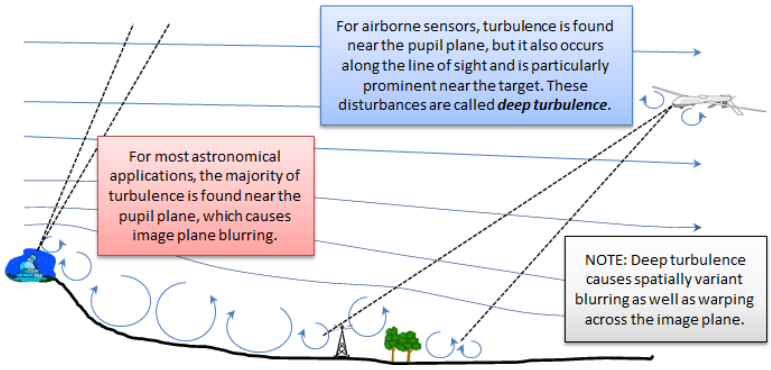

Figure 1: The Index of Refraction along an optical path to varies due to air density, moisture, temperature, and motion of atmospheric constituents, resulting in spatially variant distortions.

The desire to overcome the problems of imaging through a turbulent atmosphere has led to two general approaches for mitigating these problems, optical-mechanical and algorithmic. Optical-mechanical methods are the realm of adaptive optics, which merges optical wavefront sensing with mechanical distortion of mirror surfaces to correct the distortions in

the wavefront [3]. Algorithmic methods rely on the recording of the image in the focal plane of the optical system and the correction of the image formation distortions by computer processing of the focal plane data. The most successful of these methods for mitigating the effects of turbulence by computer processing are blind deconvolution techniques, which do not require knowledge of the instantaneous PSF that is present in the degradation of an image frame acquired by short image exposure times [4] [5] [6] [7].

Two important themes are found in blind deconvolution techniques: (1) the application of various mathematical models for the properties of the atmospheric turbulence mechanisms associated with the formation and acquisition of degraded imagery; and (2) the formulation of the blind deconvolution solution as an optimization problem. An example of the degree of sophistication associated with these methods is the modeling of atmospheric turbulence in the entrance pupil of an optical system by phase screens, using Zernike polynomials as basis functions [6]. In these methods, the optimization problem searches the space of Zernike polynomial coefficients, which are assumed (for a circular aperture) to describe the distortion of the wavefront entering the pupil plane of the optical system. Methods of this type are characterized as "blind" deconvolution because there is no known description for either the object or the PSF of the image formation process. Thus, the space of unknowns consists of the possible pixel intensities of the object and the Zernike representation coefficients of the PSF. The search for a solution is guided by embedding the unknowns associated with the PSF and object into a merit or error function, and the minimization of this merit function is achieved by an appropriate numerical method.

One of the most significant developments in signal processing in the last two decades is the development of compressive sensing. Compressive sensing technology has resulted in concurrent development and application of sparse, redundant, and over-complete representations of data and systems [8]. The core of these methods is the application of signal models that are more general than the orthogonal functions exemplified by the sine/cosine bases of Fourier theory. For example, the Wavelet Transform is more adaptive to specific characteristics of the data and is now known to have the characteristics of inducing sparsity that is very specifically "tuned" to the actual behavior of the data. Advances in image compression such as JPEG2000 exploit this property of the Wavelet Transform to achieve higher fidelity at lower compressed file sizes than previous techniques.

An important application of sparse methods is the construction of dictionaries as collections of basis functions to compose (i.e., synthesize or analyze) any arbitrary function. A number of studies have shown that the data being analyzed and processed by sparse representations can be used to construct custom dictionaries that are tuned to, and optimal for, a chosen task (see e.g., [9] [10]). The use of a custom dictionary has been applied to the problem of blind deconvolution, but only initially was done in the case of making the optimal dictionary from a single frame of imagery [9]. In many applications of atmospheric turbulence imaging it is possible to acquire many, even a large number, of image frames [11] [12] [13]. Our focus in this research is the application of sparse signal representation methods to multi-frame-blind deconvolution (MFBD), given anisoplanatic turbulent imaging conditions. This extends earlier work in this area for the isoplanatic imaging case [14]. In Ref. [1], the authors showed that resolution varies with focal plane position when imaging through turbulence, and presented a statistical analysis of the resolution as a function of telescope diameter and Fried parameter. These results extend earlier work, by Fried, and provide the motivation for pursuing a block-based approach herein. The following sections describe and demonstrate methods for using atmospheric PSFs to derive custom dictionaries, and to use those dictionaries for MFBD.

2. ASSUMPTIONS, METHODS AND PROCEDURES

2.1 Assumptions

The developments we report here, for modeling and processing of atmospheric turbulence imagery, are based on the following assumptions:

- Image formation through atmospheric turbulence may be modeled as a linear shift-variant system, i.e., as the effect of convolution of optical intensities emitted from an object using an atmospheric PSF which varies across the focal plane. Stated succinctly, we assume image formation is anisoplanatic.
- The turbulence PSF can be described by a sparse representation using a dictionary.
- The representation is said to be sparse because the number of $N \times N$ basis functions, k, used to represent the $N \times N$ PSF satisfies $k \ll N^2$.

- It is desirable that the basis used in seeking a sparse representation be over-complete, i.e., that there be redundancy in the basis set used to find the sparse representation of a signal, but this is not a requirement for the sparse representations sought hereafter.
- The basis set is designed so that it is "tuned" to the characteristics of a given data set by training on sample PSFs. We also call this a custom dictionary for the data set.

2.2 Methods

The methods of sparse representation of signals grow from both linear algebra and numerical optimization. The specific methods that we have employed in this research are described in Ref. [9]. The methods we have most significantly employed in the development of our sparse MFBD and PSF modeling are:

- *K-SVD.* One of the most effective of tools for designing a custom dictionary is the K-SVD algorithm [10]. This algorithm is a combination of K-Means clustering and the Singular Value Decomposition (SVD). The clustering portion of the K-SVD algorithm finds a sparse representation of the training data by clustering the data, and the SVD portion then updates a dictionary matrix from the most significant cluster to the least significant cluster.
- *Orthogonal Matching Pursuit (OMP).* The representation of a signal in terms of a dictionary can be difficult when the dictionary is over-complete and the representation redundant. OMP is an algorithm that extracts the best representation from a dictionary, calculating the coefficients that minimize the mean-square error in the representation of the signal in terms of the dictionary elements. This process can be applied to the case in which the dictionary is not over-complete, as well.
- *Constrained Optimization.* The problem of optimization in the case of blind deconvolution is not straightforward and must be based on optimization methods that impose constraints on the solution to enforce physical reality, e.g., positivity. We have used two constrained optimization methods in our development of blind deconvolution, a stochastic gradient descent method adapted from Ref. [15] and the well-known algorithm of Broyden-Fletcher-Goldfarb-Shanno (BFGS) [16], as implemented in the limited memory form.
- *Non-rigid image registration.* Atmospheric turbulence can cause local geometric distortions in the image frames when severe enough. Recent work has shown the value of including a preprocessing step to correct these distortions prior to the MFBD process [12] [13]. In this work, a diffeomorphic algorithm is applied for this purpose [17].

2.3 Procedures

To construct a custom dictionary of PSFs, it was necessary to have a training set of PSFs to submit to the K-SVD algorithm. This was done using a well-known wave propagation-based simulation software [18]. The simulation parameters are shown in Table 1 and Table 2. The C_n^2 value was chosen to model a medium strength atmospheric turbulence. It should be noted that this initial level of turbulence was a deliberate choice, so that concerns in developing the related MFBD algorithm would not be masked or conflated with extremely difficult turbulence conditions.

PSFs produced by the simulator were used as input to the K-SVD algorithm for the training of a custom dictionary. The parameters of the training were that each dictionary element was of the same size as the PSF images. Thus, the PSFs were processed without the using the block-overlap-and-add method that is common in K-SVD training. Figure 2 is a display of one custom dictionary obtained by this procedure. The OMP algorithm was used to construct the representation.

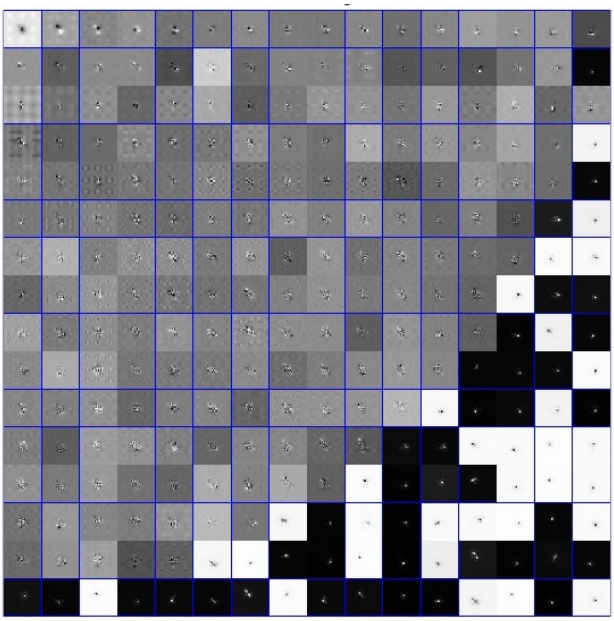

Figure 2. Custom dictionary derived using K-SVD and trained on simulated PSFs; Left: 51X51 atoms; contains 256 atoms of size 51X51; a similar one was derived for 65x65 PSFs.

Having derived a custom dictionary from the atmospheric PSFs, the next challenge was to accomplish MFBD with sparsity in the PSFs of the blind deconvolution algorithm. The value of performing blind deconvolution with multiple frames of imagery is to accumulate multiple observations of the underlying object, which is assumed to not change from frame to frame. However, there is a difficulty in using multiple frames; namely, the computational burden of processing many frames in simultaneous operations. The alternative to doing MFBD with all variables and data values, simultaneously, is to devise a way to use the information in one frame for an interim solution, then use the information in the next frame to compute a new interim solution, and continue until all frames have been processed. The cycle of processing frames in sequence, rather than in one big batch, was initially referred to as *incremental* MFBD [11]. The same concept was later re-named as *online* MFBD [15], since the processing may occur as each new frame is acquired and is suitable for processing MFBD solutions as the data arrives online, in real-time. We have adopted herein the description of "streaming" for the incremental methods that we first reported [11], in keeping with the most recent dominant terminology for on-line processes that deliver image data sets one frame at-a-time.

The online procedure of [15] was adapted to demonstrate the application of MFBD with a sparse custom dictionary. As an alternative to this method, the BFGS algorithm in its limited memory form with bounds (L-BFGS-B) was also used [16]. In either instantiation, the online procedure consists of cycles of "outer-loop" processing on each image block, and a sequence of "inner-loop" steps within each outer-loop processing of a frame. Because of the anisotropic nature of image formation in deep turbulence, and the corresponding variability of resolution on the focal plane [1], the overall process is adapted and applied to sequences of blocks extracted from the input frames. The size of the blocks is chosen so that one can assert that image formation in that local region of the focal plane is approximately isotropic.

The first step in the outer loop of processing accepts a new input frame and performs a global, non-rigid, geometric registration to remove local image warping that occurs due to local wavefront tip/tilt effects. The well-established MATLAB function *imregdemons* was chosen for this step [17]. A reference frame, derived from averaging several input frames, is maintained throughout the process to support the registration of each new frame. After registration, the new frame is broken down into contiguous blocks. Each block with a surrounding overlap region is extracted from the frame. In this work, the combination of block and overlap is referred to as a *computational patch*.

As each new computational patch is received, the sequence of inner-loop steps applied consists of:

- An initial guess for the object computational patch is fixed using the computational patch data from the first frame. (After the first frame, the object computational patch estimate produced by the previous inner loop iteration

is carried forward.) An initial guess for the PSF is also fixed as a Gaussian function with width equal to an estimate of the time averaged PSF for a typical turbulent atmosphere condition.

- With the object computational patch fixed, a series of iterations are performed to successively refine the estimate of the PSF for that patch. These iterations project changes onto the estimate of the PSF, chosen to follow the stochastic gradient of the data consistency criterion [15] or the analytical gradient used by L-BFGS-B.
- At one or more points between adjustments to the PSF estimate, the PSF estimate at that point is represented sparsely with the custom dictionary created earlier. This serves to suppress aspects of the PSF estimate that are not consistent with signal properties learned during dictionary training.
- After several adjustments to the current PSF estimate, the PSF is fixed and a corresponding series of changes is made to the object computational patch estimate using either the algorithm of Ref. [15] or BFGS. The deliberate act of taking an estimate of the PSF, and then restructuring it to be sparse in the representation of the custom dictionary, is the procedure by which we have chosen to produce MFBD with sparse properties for the PSFs.
- The cycling in this manner continues until either a stopping criterion or a pre-defined total number of iterations is satisfied.
- This completes the inner loop cycling iterations on one computational patch. A new step begins in the outer-loop by extracting the corresponding patch from a new frame. The inner loop cycling of this new patch begins with the object estimate carried over from the previous frame, and a PSF estimate is generated as described above.
- Cycling now continues, as before, until all computational patches from all frames have been processed. At this point, a final object estimate is formed by extracting the contiguous blocks from the object computational patch estimates and reassembling them into a mosaic image. The implementation includes several options for smoothing at the block boundaries.
- It is possible to terminate or resume operations with the results from the previous full outer loop cycle.

The imposition of the sparse properties for the PSF was associated with substantial reduction in the error in MFBD reconstruction of an object. Dictionary processing is not used during adjustment of the object at the present time, although it could be of value for denoising or suppressing artifacts in the object estimate [14] [19].

Table 1. Simulation Parameters (Optical)

Parameter	Value
Aperture (m)	0.3556
Focal length (m)	3.9100
F-number	10.9955
Wavelength (microns)	7.8500e-07
Object distance (m)	2450
Nyquist pixel spacing (microns)	4.3157
Cutoff frequency (cycles/mm)	115.86

Table 2. Simulation Parameters (Turbulence)

Parameter	Value
C_n^2 ($m^{-2/3}$)	2.0000e-15
Theoretical r_0 (m)	0.0959
Isoplanatic angle (pixels)	11.1458
RMS tilt (pixels)	2.5440

3. RESULTS AND DISCUSSION

The representation of a turbulent atmosphere PSF in a sparse form is not a surprise, when considered in the context of the state-of-art in simulation turbulent PSFs. The ability of existing software to represent and simulate turbulent PSFs with the Zernike polynomial expansion is demonstration of a sparse representation. Experimental evidence in this area has shown that the greatest amount of wavefront distortion occurs in the lowest order of the Zernike polynomial coefficients, i.e., piston error (focus) and wavefront tip-tilt [20]. The advantage of the use of a custom dictionary is that the basis functions used in the dictionary are not derived from generic functions, such as the discrete cosine transform or the various wavelets, but are directly compiled from the statistics of a set of PSFs. This means that the custom dictionary has properties that relate more closely to actual statistical models of a family of turbulent PSFs and can be used to represent, with great accuracy, any other PSF possessing the same turbulent statistics.

The streaming MFBD algorithm described above was tested by using a set of simulated imagery. The level of turbulence is significant in this simulation and produces significant local geometric distortion due to wavefront tip/tilt. The left side of Figure 3 shows examples of the PSFs generated by the wave propagation code where the value of D/r_0 is approximately 3.7. A spatio-temporal average of 10,000 PSFs was used to compute an estimate of the long-term optical transfer function (OTF). This estimate is shown alongside the theoretical diffraction limited OTF in the right side of Figure 3. PSFs across the focal plane are not statistically independent, and this shows up in the extended tail seen in this plot.

To test restoration performance of the MFBD algorithm, an image of a harbor scene was processed using the wave propagation-based turbulence simulator to generate sequences of degraded image frames. The streaming algorithm was then cycled as described above using the custom dictionary. In seeking to characterize the differences in algorithmic optimization performance, noise has not been included in these simulations.

The important parameters governing the MFBD process are shown in Table 3. In the table, "Algorithm 1" refers to the algorithm of Ref. [15], while "Algorithm 2" refers to MFBD using L-BFGS-B.

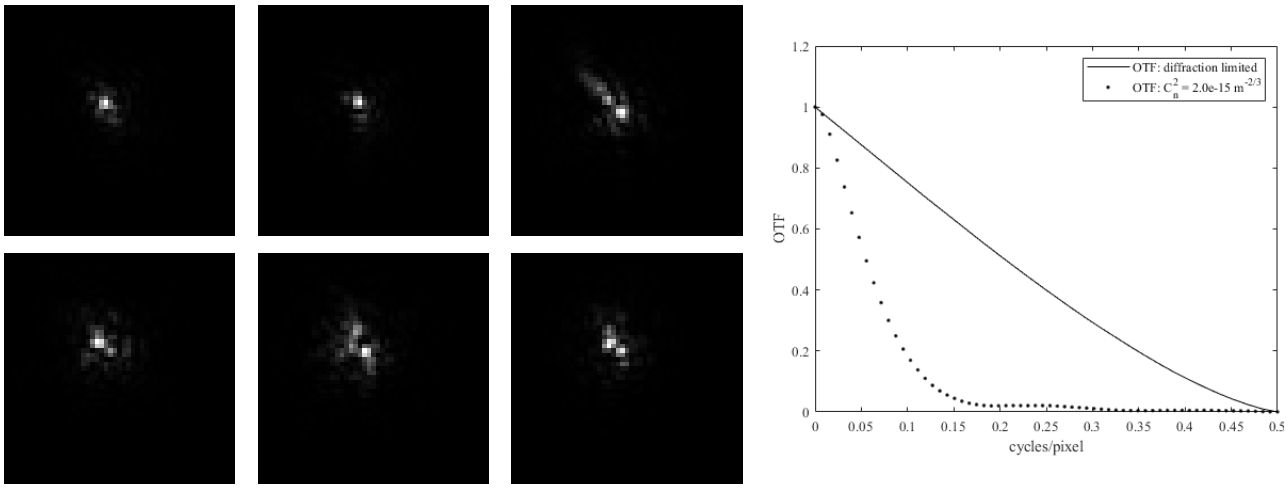

Figure 3. At left, six sample PSFs produced by the wave propagation simulator of Ref. [18]. At right, a comparison of the OTF estimate produced by spatio-temporal averaging of 10,000 simulated PSFs over several frames and the diffraction-limited OTF.

Table 3. Main processing parameters for the MFBD algorithm

Parameter	Algorithm 1	Algorithm 2
Overlap	51	72
Block size	16	16
PSF size	51	65
Iterations (PSF)	500	250
Iterations (Object)	5	3
OMP coefficients[1]	24	24
Sparsity interval[2]	400	200
Noise	None	None

[1] "OMP coefficients" refers to the number of dictionary coefficients solved for by OMP in the sparse representation.

[2] "Sparsity interval" refers to how often a sparse representation is sought during the PSF updates, e.g., for a setting of 400, only once at iteration 400 if the total Iterations (PSF) is 500.

Given a block size of 16X16, the resulting computational patch size is 118X118 for an overlap of 51 and is 160X160 for the overlap of 72, used in the L-BFGS-B case. The overlap was chosen to be at least as large as the PSF size to include enough image data to avoid padding issues. Many different combinations of the above parameters have been explored in a wide-ranging parameter study. We observed that the algorithm of Ref. [15] can accept more frequent sparsity processing without disrupting convergence, whereas the L-BFGS-B algorithm can exhibit divergence if the frequency of sparsity processing is too high. The two algorithms have different sensitivities to the above parameters, and these parameter sets were chosen from among the "best cases" from the parameter study.

Figure 4 shows the result of reconstructing these images with MFBD Algorithm 1. The left is the original object, the center is the raw, unprocessed 10th frame, and the right is the reconstruction after frame 10 using the algorithm of Ref. [15]. The scene is recognizable, although there is significant loss of detail and small structure in the turbulent imagery. Figure 5 shows a similar result for MFBD Algorithm 2. The restored image in each case is clearly an improvement and much of the degradation caused by the turbulence has been mitigated. Because of the large number of cases in the parameter study, the processing was limited to 10 frames. Processing more frames should serve to improve the results further.

Figure 4. Results for Algorithm 1 using the parameters in Table 3 after 10 frames: (left) the reference object; (center) the unprocessed 10th frame; and (right) the restored image (cropped to eliminate border effects produced by the global registration processing)

Figure 5. Results for Algorithm 2 using the parameters in Table 3 after 10 frames: (left) the reference object; (center) the unprocessed 10^{th} frame; and (right) the restored image (cropped to eliminate border effects produced by the global registration processing)

Since visual comparisons are sometimes deceiving (human perception is simultaneously very forgiving of some characteristics and unduly harsh about others), Table 4 summarizes the result of calculating image quality metrics from the results of the MFBD processing. The following four metrics are included in the table:

- IMMSE: image mean-square error
- PSNR: peak signal-to-noise ratio
- SSIM: structural similarity index measure
- MS-SSIM: multiscale structural similarity index measure

All of these are available and documented as part of the MATLAB Image Processing Toolbox. For all but IMMSE, larger values are preferred, with SSIM and MS-SSIM being confined to the interval [0,1].

The first row in the table shows the metrics computed using 200 raw unprocessed frames, with 2σ bounds. The second row shows the quantitative benefits of the global registration process over the same 200 frames, again with 2σ bounds. The remaining four rows show the values resulting from running the algorithms using the parameters from Table 3. MFBD results are shown first without the dictionary applied and compared to results with one sparse dictionary call for each algorithm. These results support the assertion that incorporating the dictionary sparse representation in the MFBD process offers both qualitative and quantitative improvements.

Table 4. Image quality metrics for 10 input frames (best case in bold face)

Mitigation	IMMSE	PSNR	SSIM	MS-SSIM
Raw	0.0308 ± 0.0183	15.2914 ± 2.4357	0.3987 ± 0.1915	0.6004 ± 0.2749
Registered	0.0172 ± 0.0038	17.6680 ± 0.9247	0.5799 ± 0.0745	0.7970 ± 0.0584
Algorithm 1	0.0091	20.4100	0.7588	0.9151
Algorithm 1 - Sparse	**0.0076**	**21.1950**	**0.7890**	**0.9374**
Algorithm 2	0.0096	20.1610	0.7439	0.9072
Algorithm 2 - Sparse	0.0082	20.8540	0.7770	0.9275

4. SUMMARY

The advantage of sparse representations has been demonstrated repeatedly in signal processing during the past decade. The application sparse dictionary representations is also valid for the problems of atmospheric turbulence and MFBD. We find that:

- Custom dictionaries of PSFs, derived using K-SVD, can be used in the development of MFBD algorithms, including incremental or online algorithms applicable to the solution of image frames acquired in real time. The only limitation to real time application is the available computation power to keep pace with the incoming image data rate.
- Sparsity in the reconstruction process is a valuable contribution to producing an improved result for MFBD. Based on these limited results, we speculate, but have not proven, that the improvement is due to the optimization process having fewer opportunities for error, because the custom dictionary is better matched to the statistics of the turbulent PSFs that produced the imagery.
- Block-based MFBD processing is an effective means of dealing with the anisotropic blur, and the variability of resolution on the focal plane, introduced by deep turbulence.
- The differences in quality produced by the algorithm of Ref. [15] and L-BFGS-B are small, and further effort is needed to find optimal parameter settings for each of them. We can draw no conclusion at this point as to which is better.

Future work will be focused on understanding the performance of our mitigation approach in the presence of noise and computationally efficient implementations using parallel architectures.

ACKNOWLEDGEMENT: The authors gratefully acknowledge the financial support of the US Air Force Research Laboratory under contract #FA8650-18-C-1017 and the collegial support of Dr. Russell Hardie in providing the simulated data for results reported herein. The content of this paper has been approved for public release through PA Approvals AFRL-2021-2208 and AFRL-2021-2309.

5. REFERENCES

[1] B. R. Hunt, A. L. Iler and D. G. Sheppard, "Lucky Imaging and Local Resolution Statistics for Atmospheric Turbulence Characterization - Winner of the 2021 KBR Technical Journal Gold Medal," *KBR Technical Journal,* vol. 1, 2021.

[2] M. C. Roggemann and B. M. Welsh, Imaging Through Turbulence, Boca Raton: CRC Press, 1996.

[3] J. M. Beckers, "Adaptive Optics for Astronomy: Principles, Performance, and Applications," *Annual Review of Astronomy and Astrophysics,* vol. 31, no. 1, pp. 13-62, 1993.

[4] E. Pantin, J.-L. Starck and F. Murtagh, "Deconvolution and blind deconvolution in astronomy," in *Blind Image Deconvolution*, Boca Raton, CRC Press, 2007, pp. 277-316.

[5] A. Cornelio, E. Piccolomini and J. Nagy, "Constrained numerical optimization methods for blind deconvolution," *Numerical Algorithms,* p. 23–42, 2014.

[6] C. Matson and K. Borelli, "Parallelization and Automation of a Blind Deconvolution Algorithm," in *HPCMP-UGC '06: Proceedings of the HPCMP Users Group Conference*, Denver, 2006.

[7] F. Sroubek and J. Flusser, "Multichannel blind iterative image restoration," *IEEE Transactions on Image Processing,* p. 1094–1106, 2003.

[8] M. Candes and M. Wakin, "An introduction to compressive sampling," *IEEE Signal Processing Magazine,* pp. 21-30, 21 March 2008.

[9] M. Elad, Sparse and Redundant Representations: From Theory to Applications in Signal and Image Processing, New York: Springer, 2010.

[10] M. Aharon, M. Elad and A. Bruckstein, "K-SVD: An algorithm for designing overcomplete dictionaries for sparse representation," *IEEE Transactions on Signal Processing,* pp. 4311-4322, 2006.

[11] D. G. Sheppard, B. R. Hunt and M. W. Marcellin, "Iterative multiframe superresolution algorithms for atmospheric-turbulence-degraded imagery," *Journal of the Optical Society of America A,* pp. 978-992, 1998.

[12] R. C. Hardie, M. A. Rucci, A. J. Dapore and B. K. Karch, "Block matching and Wiener filtering approach to optical turbulence mitigation and its application to simulated and real imagery with quantitative error analysis," *Optical Engineering,* 2017.

[13] M. A. Hoffmire, R. C. Hardie, M. A. Rucci, R. Van Hook and B. K. Karch, "Deep learning for anisoplanatic optical turbulence mitigation in long-range imaging," *Optical Engineering,* 2021.

[14] B. R. Hunt and K. Knox, "Optimal Dictionaries for Sparse Solutions of Multi-frame Blind Deconvolution," in *Advanced Maui Optical and Space Surveillance Technologies Conference*, Wailea, 2014.

[15] M. Hirsch, S. Harmeling, S. Sra and B. Scholkopf, "Online multi-frame blind deconvolution with super-resolution and saturation correction," *Astronomy & Astrophysics,* 2011.

[16] C. G. Broyden, "The Convergence of a Class of Double-rank Minimization Algorithms 1. General Considerations," *IMA Journal of Applied Mathematics,* p. 76–90, 1970.

[17] "imregdemons," The Mathworks, [Online]. Available: https://www.mathworks.com/help/images/ref/imregdemons.html. [Accessed 14 06 2021].

[18] R. C. Hardie, J. D. Power, D. A. LeMaster, D. R. Droege, S. Gladysz and S. Bose-Pillai, "Simulation of anisoplanatic imaging through optical turbulence using numerical wave propagation with new validation analysis," *Optical Engineering,* 2017.

[19] B. R. Hunt, A. L. Iler, C. A. Bailey and M. A. Rucci, "Synthesis of atmospheric turbulence point spread functions by sparse and redundant representations," *Optical Engineering,* vol. 57, no. 2, February 2018.

[20] F. Roddier, M. Northcott and J. E. Graves, "A simple low-order adaptive optics system for near-infrared applications," *Publications of the Astronomical Society of the Pacific ,* pp. 131-149, 1991.